Chapter 5

Robust Diabetic Retinopathy Detection Using Twin Support Vector Machines

In the previous chapter, a robust TSVR was presented and the test results were reported for both synthetic and real benchmark data. In this chapter, the classification variant of TSVR, twin support vector machine (TWSVM), is modified to provide robustness. TWSVM is used here for the important application of DR detection. Like TSVR, TWSVM is also four times faster than SVM [32]. In the work being reported here, a robust loss function was used with TWSVM. Towards this direction, first, the introduction of diabetic retinopathy is given, followed by its literature survey.

It is essential to get a regular checkup of our eyes so that the earlier detection of diabetic retinopathy can be made possible. This is a disease that occurs due to retinal damage, which results in prolonged occurrence of diabetic Mellitus. The detection of DR using eye fundus images has been a current research topic in medical and vision processing. There are varieties of methods developed to automate the process of DR detection. Researchers have made use of diverse types of classifiers to detect the pres-

ence of DR accurately. SVMs contributed to the latest modeling of DR detection. That proved to be an efficient technique but still time-consuming, especially when the dataset is huge. Further, there is a noticeable decrease in the performance of SVM when the data set is corrupted by noise or outliers. This was the motivation to propose the twin support vector machine (TWSVM) and its robust variants for the DR detection task. This work involves feature extraction from the digital fundus images and subsequent classification using the TWSVM and its robust variants. The comparison with the previous results of SVM illustrated the superiority of our model. It should be noted that this classifier choice solved the problem of high computational time and made the DR detection robust.

5.1 Introduction

As reported by WHO [108], the 7th leading reason of death worldwide is diabetes. Diabetic patients tend to show the abnormality in their retina. As the disease progresses slowly, it is suggested by the medical experts that diabetic patients should refer to the doctors at least twice a year so that the signs of an eye-related illness can be timely diagnosed. When performed manually by specialists, this process is time-consuming and expensive. Furthermore, the increasing number of diabetic patients leads to a lack of medical resources in some parts of the world. This may lead to visual loss, which can never be reversed. Also, if the patient is in the early stage of DR, detection and immediate treatment can control the disease. Therefore, it is essential to get the required diagnosis on time. Sometimes, the manual diagnosis cannot be trusted entirely as the lack of experience may lead to misdiagnosis. In such cases, the computer-aided diagnosis works better. Therefore, to get a fast and reliable DR diagnosis, one can utilize the computer-aided diagnosis.

The DR starts as minor anomalies in the retinal capillaries. The very first abnormality is the presence of Microaneurysms (Ma) (Figure 5.2) which leads to the

rupture of intra-retinal hemorrhage. This disease's severity can be classified as mild non-proliferative diabetic retinopathy (NPDR) when the microaneurysms are seen for the first time in the retina. The subsequent abnormality that arises is hard exudates (Figure 5.1) and retinal edema. This leads to increased permeability through the capillary walls. The next stage is the moderately proliferative DR (MPDR), in which hard exudates start leaking because of weak blood vessels. The last stage is the proliferative DR (PDR), in which the blood vessels disrupt and leads to microinfarcts in the retina [108]. These microinfarcts are known as soft exudates (SE) (Figure 5.3) [2].

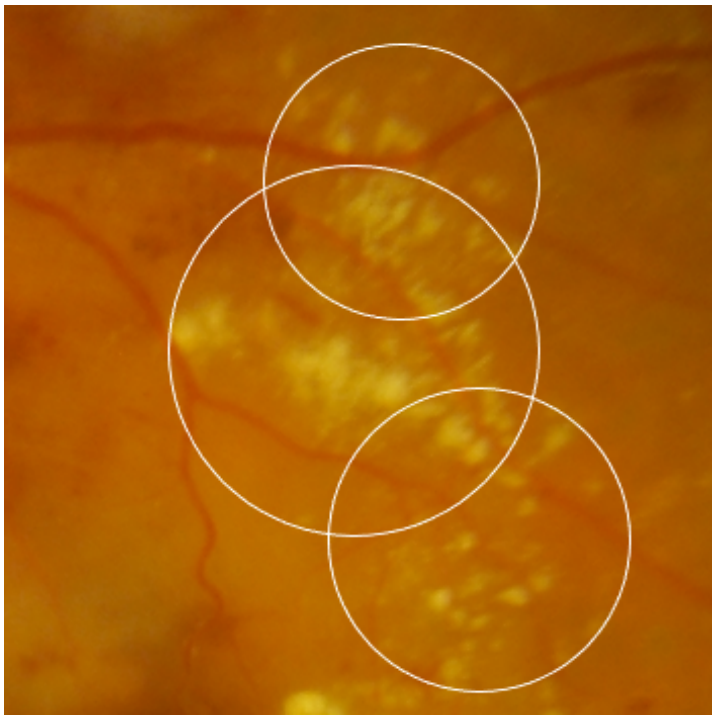

Figure 5.1: Hard Exudates [2]

5.1.1 Motivation and Contributions

Various researchers have worked to automate the process of DR detection so that misdiagnosis can be prevented. As the problem is related to classifying the cases into diabetic and non-diabetic, the researchers have used various classifiers to enhance the quality of DR detection. These classifiers work well when the dataset is small, but model training

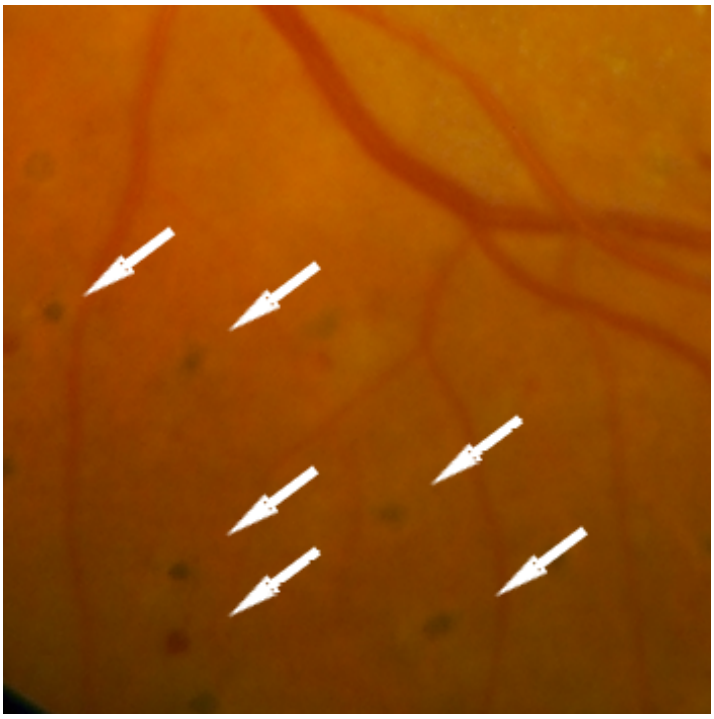

Figure 5.2: Microaneurysms [2]

takes too long and makes the overall processing slow when the dataset is large. This calls for a faster classifier that can train the model faster compared to other standard classifiers. Since TWSVM is four times faster than the conventional SVM [32], it is proposed to use TWSVM for DR detection.

The significant contributions to this work are listed below:

1. TWSVM was used as the classifier to solve DR detection because the computational time taken by TWSVM is less.

2. The robust variant of TWSVM, pin-TWSVM, was also used to add robustness to our model. In this variant, the pinball loss function, incorporated with TWSVM, was used for robust DR detection.

3. In this work, only eight features were extracted from the images to detect diabetic retinopathy in the images. These features are a number of microaneurysms, area of microaneurysms, the standard deviation of red, green, and blue components,

Figure 5.3: Soft Exudates [2]

the entropy of the green part of an image, density of hard exudates, and the density of blood vessels.

5.2 Related work

In this section, we discuss literature that has contributed to DR detection. DR detection using machine learning has currently been an interesting research area, and many research proposals are trying to tackle this problem using machine learning approaches. Towards this direction, first is the computer-aided screening system designed in 2013 that analyzed the fundus images and generated the report of its severity for DR [109]. In that work, classifiers like the Gaussian mixture model (GMM), SVM, Adaboost, and k-nearest neighbor (KNN) were used for classifying retinopathy lesions. They observed that GMM and KNN were the best classifiers for red and bright lesions classification [109].

Similarly, the use of GMM was further extended in this area using the three-stage

segmentation algorithm [110]. In that work, eight features were extracted and were passed through the pre-processing and post-processing stages defined in [110]. The algorithm managed to achieve an accuracy of 95.2%, 95.3% and 95.15% over DRIVE [111], CHASE-DB1 [112], and STARE [113] data sets respectively.

In 2015, the STARE dataset was used further to test another iterative algorithm, which was proposed in [114]. In that work, Roychowdhury et al. have proposed a new algorithm that was robust to the rate of new vessel pixel addition. They reported that their method was computationally efficient and consistent throughout its performance [114].

Another work that used morphological operations together with machine learning also grabbed attention. In that work, after pre-processing, Lachure et al. [115] applied some morphological operations to find the microaneurysm. After that, they extracted the features and trained the classifiers. They used SVM, and KNN [115] in that work and the authors observed that SVM performed better than KNN. In 2016, the detailed analyses of DR detection using machine learning were provided in [116]. The work provided a detailed survey on DR detection using machine learning models.

Furthermore, another work proposed in [117] emphasized the data pre-processing by applying histogram equalization, green channel extraction, image enhancement, and resizing techniques. They used the Kaggle DR dataset. That work proved that accurate pre-processing methods lead to better accuracy of a model.

Another important contribution in this area was provided in [118]. In that paper, Kumar et al. [118] found that only two features, area, and the number of microaneurysms were sufficient to predict the DR in the fundus images. That work was also shown to be computationally efficient. Similarly, segmentation techniques were also applied to the DR detection problems in [119].

In the next section, we describe the data set used in this chapter to demonstrate the effectiveness of the proposed method.

5.3 Dataset Used

In this work, the DIARETDB1 – dataset [3] was used, which was obtained from the standard diabetic retinopathy database. This dataset comprises 89 colored eye images. Amongst these, 84 contain mild symptoms of the DR, and the rest five are normal as these do not have any of the above-discussed abnormalities. This shows that the data set has a huge class imbalance. Similarly, the dataset contains 89 already extracted microaneurysms images and 89 already extracted hard exudates images [3].

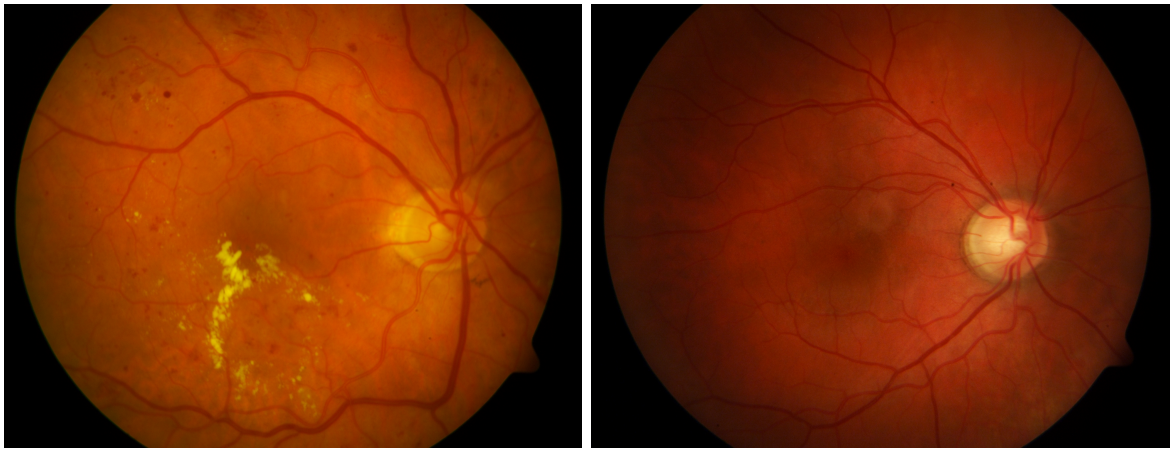

(a) Diseased Image (b) Normal Image

Figure 5.4: Figure Showing the Eye Fundus Images of the Diseased Person and the Normal Person [3]

5.3.1 Feature Extraction

In this work, eight features were extracted from the data set. The flow chart given in Figure 5.5 illustrates the steps followed in extracting the features. The features which were used in this work are given below:

1. Number of Microaneurysms
2. Area of Microaneurysms
3. The red components's standard deviation

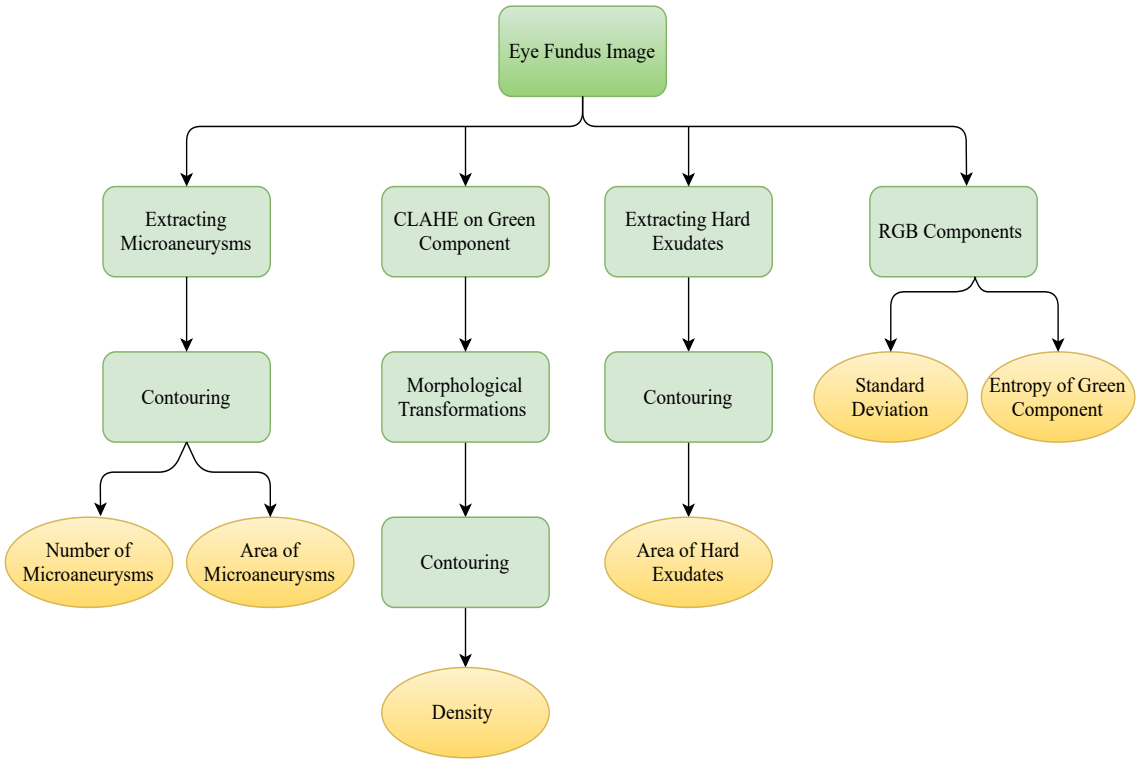

Figure 5.5: Figure Showing the Steps Followed To Extract The Features From the Eye Fundus Images; The Bottom Circles Represent The Features Used In This Work

4. The green component's standard deviation
5. The blue component's standard deviation
6. The entropy of green component of image
7. Hard exudates' density
8. The density of blood vessels

Next, the detailed feature extraction is described in the subsequent subsections.

5.3.2 Number and Area of Microaneurysms With a Density of Hard Exudates

Inspired by the work of [118], the two features, namely, number and area of microaneurysms, were also used in this work. Towards this direction, first, the microa-

neurysms' edges were obtained using contours, and the area then filtered these contours. Contours with large areas were removed. The Remaining contours were used to find the number and area of the microaneurysm. In this way, the first two features were obtained from the data set. These steps were also used to calculate the area of hard exudates. On dividing it by the total area, the density of the hard exudates was obtained.

5.3.3 Blood Vessels Extraction

In this subsection, the steps are described for the blood vessels extraction.

1. First, the adaptive histogram equalization ADHE [120] was applied to the image's green component. This reduces the problem of noise amplification in the images.

2. Next, the morphological opening-closing operations were applied three times on different size kernels to remove the noise.

3. To further reduce noise, binary thresholding [121] was applied.

4. Using contours, the image was filtered using the area and perimeter to remove circular structures that were not blood vessels.

5. The final image was then dilated.

5.3.4 Entropy

Entropy is the measure of randomness [122]. In image processing, entropy is used to classify textures; a particular texture has one specific entropy as specific patterns repeat themselves in approximately certain ways. So, this helped in categorizing images. The formula for entropy is given by

$$H\left(s_m\right) = -\sum_{n=1}^{256} p_n\left(s_m\right) \cdot \log_2\left(p_n\left(s_m\right)\right), \ m = 1, \ldots, M \tag{5.1}$$

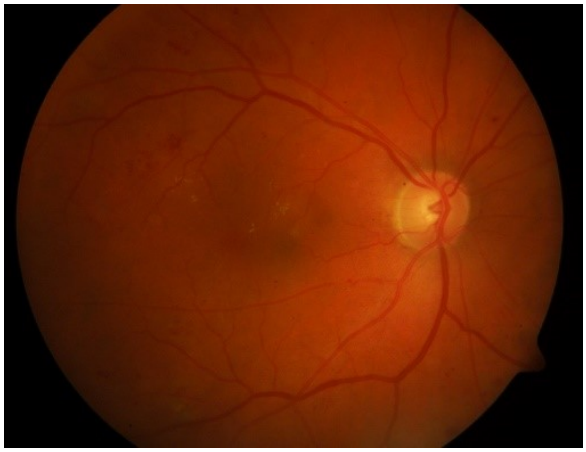

(a) Original Image

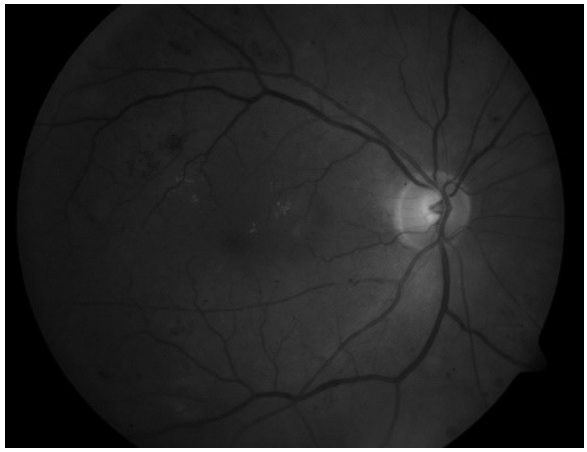

(b) Green Component of an Image

(c) CLAHE

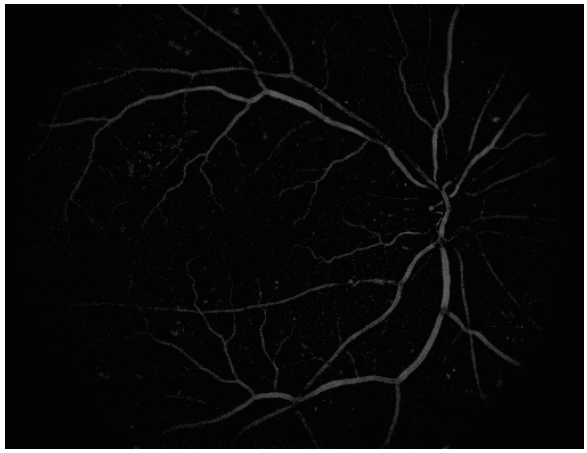

(d) Noise Reduced Image

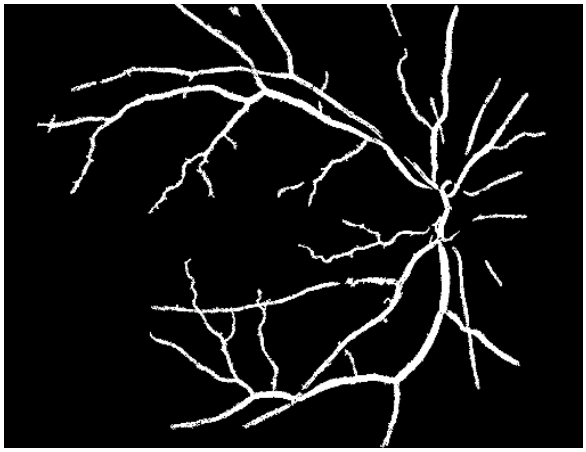

(e) Dilated Final Image

Figure 5.6: Figure Showing Effect of The Steps Applied to the Original Image to Obtain the Final Image

where $s_1, s_2, \ldots, s_m$ are the events occurring with probabilities $p(s_1), p(s_2), \ldots, p(s_m)$.

5.3.5 Standard Deviation

Next is the standard deviation. It gives the measure of variability from the mean value of pixel intensities. The high value of standard deviation confirms that the values are dispersed more from the mean, and a lower standard deviation shows that the values are close to the average value. The equation of standard deviation is given by [123]

$$\sigma^2 = \frac{1}{N-1} \sum_{i=0}^{N-1} (x_i - \mu)^2, \tag{5.2}$$

where N denotes the number of samples, μ is the mean for x input images.

5.3.6 Morphological Transformations

Morphological operations include basic operations like dilation and erosion. These operations are applied to the binary images. Two kinds of inputs are required to perform these operations, including the original image and the kernel. The kernel is also called the structuring element of an image which decides the nature of the process. Besides dilation and erosion, several other variants of morphological operations are opening, closing and gradient, etc.

5.4 Classifiers Used

In this work, the classifiers used are SVM, TWSVM, and modified TWSVM with pinball loss function. SVM and TWSVM are already described in Chapter 1. The description of TWSVM with pinball loss function is given below.

(a) Twin Support Vector Machine using pinball loss function

In this classifier, the hinge loss function from the standard TWSVM is replaced

by the pinball loss function to introduce robustness towards the noise. The conventional TWSVM is given by

$$\begin{aligned} \min_{w_1,b_1,q} \ & \frac{1}{2}(A_1w_1 + e_1b_1)^T(A_1w_1 + e_1b_1) + c_1e_2^Tq \\ \text{subject to } & -(A_2w_1 + e_2b_1) + q \geq e_2,\ q \geq 0, \end{aligned} \tag{5.3}$$

for TWSVM 1. While TWSVM2 is given by

$$\begin{aligned} \min_{w_2,b_2,q} \ & \frac{1}{2}(A_2w_2 + e_2b_2)^T(A_2w_2 + e_2b_2) + c_2e_1^Tq \\ \text{subject to } & -(A_1w_2 + e_1b_2) + q \geq e_1,\ q \geq 0. \end{aligned} \tag{5.4}$$

In (5.3) and (5.4), w_1, w_2 and b_1, b_2 are the weight vectors and bias terms for TWSVM1 and TWSVM2. The two matrices A_1 and A_2 represent the data points belonging to two different classes. The loss is represented by q in both the equations. In the conventional TWSVM, the loss function used is hinge loss function. In (5.3) and (5.4), c_1, c_2 and e_1, e_2 are the regularizers used and the vector of ones respectively.

As TWSVM with hinge loss is sensitive to outliers. The new TWSVM was proposed, which replaced the hinge loss function with pinball loss function [65] as the pinball loss function is robust to noise and outliers. TWSVM1 and TWSVM2 with pinball loss function are given by

$$\begin{aligned} \min_{w_1,b_1,\xi} \ & \frac{\nu_1}{l_2}(A_1w_1 + e_1b_1)^T(A_1w_1 + e_1b_1) + \frac{c_1}{l_1}\xi \\ \text{subject to } & (A_1w_1 + e_1b_1) \geq 0 - \xi, \\ & (A_1w_1 + e_1b_1) \leq 0 + \frac{1}{\tau_1}\xi, \end{aligned} \tag{5.5}$$

and

$$\begin{aligned} \min_{w_2,b_2,\xi} \ & \frac{\nu_2}{l_1}(A_2w_2 + e_2b_2)^T(A_2w_2 + e_2b_2) + \frac{c_2}{l_2}\xi \\ \text{subject to } & -(A_2w_2 + e_2b_2) \geq 0 - \xi, \\ & -(A_2w_2 + e_2b_2) \leq 0 + \frac{1}{\tau_2}\xi, \end{aligned} \tag{5.6}$$

respectively. In (5.5) and (5.6), ξ is the slack vector corresponding to the pinball loss function. The pinball loss function is given as follows, which can be regarded as a generalized L_1 loss:

$$L_{\text{pin}}(u) = \begin{cases} u & u \geq 0 \\ -\tau u & u < 0 \end{cases} \tag{5.7}$$

where $u = y(w^T x + b)$ with w and b are the weight vectors and bias term respectively for x input data with labels y. In (5.5) and (5.6), $\nu_1, \nu_2 > 0$ and τ_1, τ_2 are the parameters of the pinball loss function. Note that l_1 and l_2 are the number of instances in A_1 and A_2 respectively. The hinge loss function and the pinball loss function are shown in Figure 5.7 and 5.8 respectively.

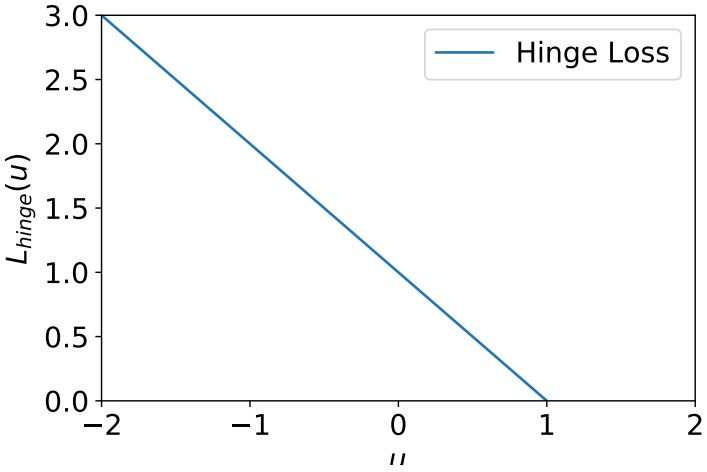

Figure 5.7: The Conventional Hinge Loss Function

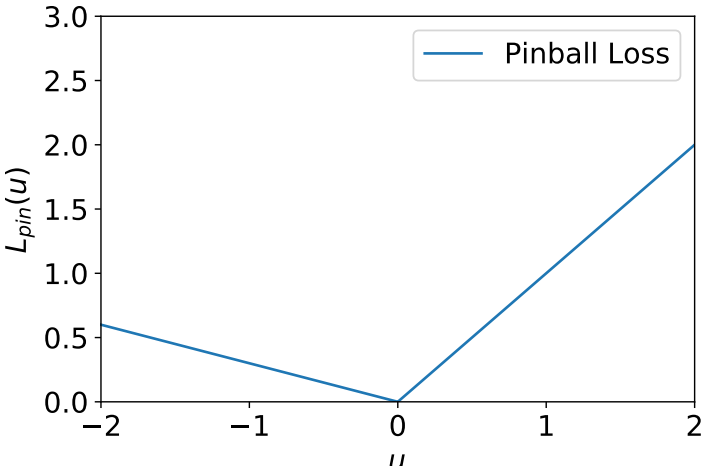

Figure 5.8: Pinball Loss Function

In Figure 5.8, the pinball loss function is shown with $\tau = 0.3$. It can be observed that the function is always positive, and the minimization of this function delivers the optimal quantile. Therefore, the function is robust towards the noise. Next, TWSVM is four times faster than SVM, and hence the resulting classifier of this problem was computationally efficient than SVM. Also, the presence of noise in the dataset severely affects the performance of the classifier; therefore, the introduction of the pinball loss function with TWSVM to the problem of DR detection has made the model robust to such noises.

(b) Gaussian Noise

Gaussian noise is the statistical noise that incorporates a probability density function (PDF) corresponding to the normal distribution function, which is also known as the Gaussian distribution. The probability distribution function, N_G of a Gaussian random variable x is given by

$$N_G(x) = \frac{1}{\sigma\sqrt{2\pi}} e^{-\frac{(x-\mu)^2}{2\sigma^2}}, \tag{5.8}$$

where x represents the grey level, μ is the mean value, and σ is the standard

deviation.

In the next section, the numerical experiments and the results are presented on the DIARETDB1 data set.

5.5 Numerical Experiments and Results

SVM, TWSVM, and the modified TWSVM with pinball loss function are compared on the DIARETDB1 data set in this section. Towards this direction, first, the features were extracted from the DIARETDB1 data set. To extract the features, the steps mentioned in Subsection 5.3.1 were followed. After obtaining the features, the data set was divided into the ratio of 80:20, where 80% data was used for the training, while 20% used for model testing. Please note that since there are only five normal eye fundus images and the rest are diseased, the data set has an extreme class imbalance in it.

5.5.1 Results On DIARETDB1 Data Set (Without Noise)

In this part of the chapter, the above-described classifiers are compared based on the accuracy over various regularization parameters. It should be noted here that no Gaussian noise was added in the feature set to test the robustness till this point. For these experiments, the regularization parameter, λ, was considered in the range of 1 to 200. Figure 5.9 shows the plot of 'Accuracy versus Regularization Parameter' for all the classifiers. 'Regularization Parameter' is plotted on the x-axis, and the 'Accuracy' is plotted on the y-axis. From Figure 5.9, it can be observed that the TWSVM with pinball loss function shows better accuracy as compared to the rest of the classifiers. Also, the plot of TWSVM with pinball loss function shows less variation with different regularization parameters while this is not so with the other classifiers. Thus, the proposed model is less sensitive to the choice of the regularization parameter. The plot is shown in red, and the highest accuracy corresponding to TWSVM with pinball loss

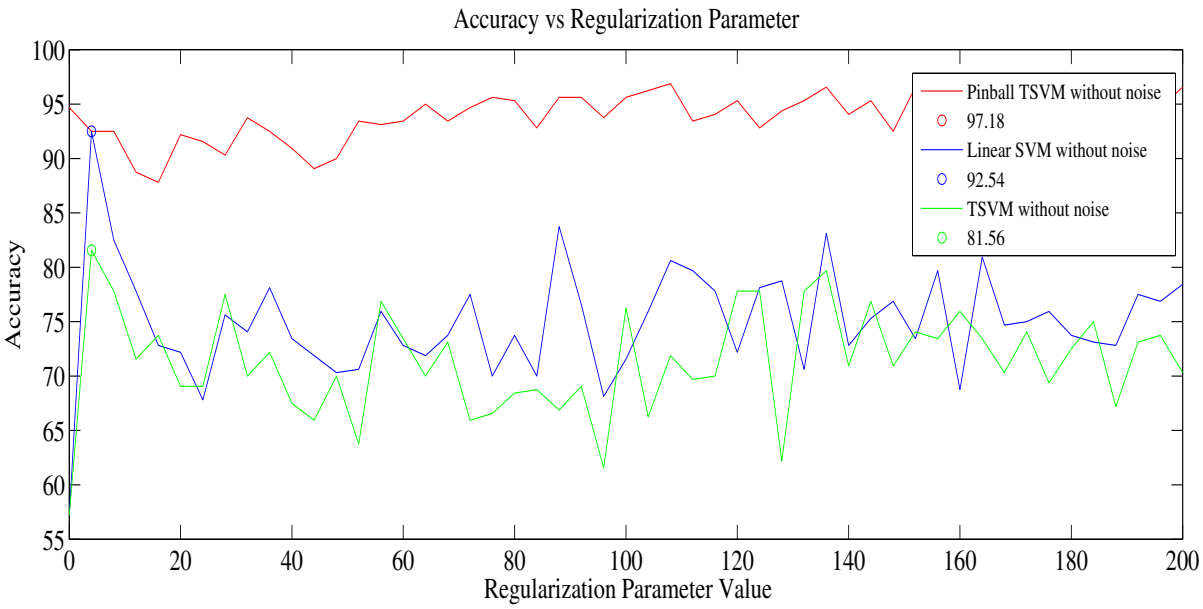

Figure 5.9: Plot of Accuracy versus Regularization parameter Without Adding Noise to The Data Set

function reported was 97.18. Another observation is that the linear SVM performed better than the conventional TWSVM on the DIARETDB1 data set when the data set was noise-free but both SVM and TWSVM show significant variation in accuracies with different regularization parameters. This establishes that the proposed model the accuracy is less sensitive to the regularization parameter choice.

5.5.2 Results On DIARETDB1 Data Set (With Gaussian Noise)

Next, the Gaussian noise was added to the DIARETDB1 data set to test the robustness of the classifiers mentioned above. Figure 5.10 show how accuracy varies against the regularization parameter after adding noise to the data sets. Please note that the Gaussian noise was added to the extracted features of the training set. Figure 5.10 shows that the accuracy of all the classifiers decreased to some extent, but the decrease for TWSVM with pinball loss function was much less compared to the rest of the approaches. These experiments were also used for hyperparameter tuning to obtain the best suitable hyperparameters for different classifiers on the DIARETDB1 data

set. TWSVM with pinball loss function shows significantly less variation in accuracies

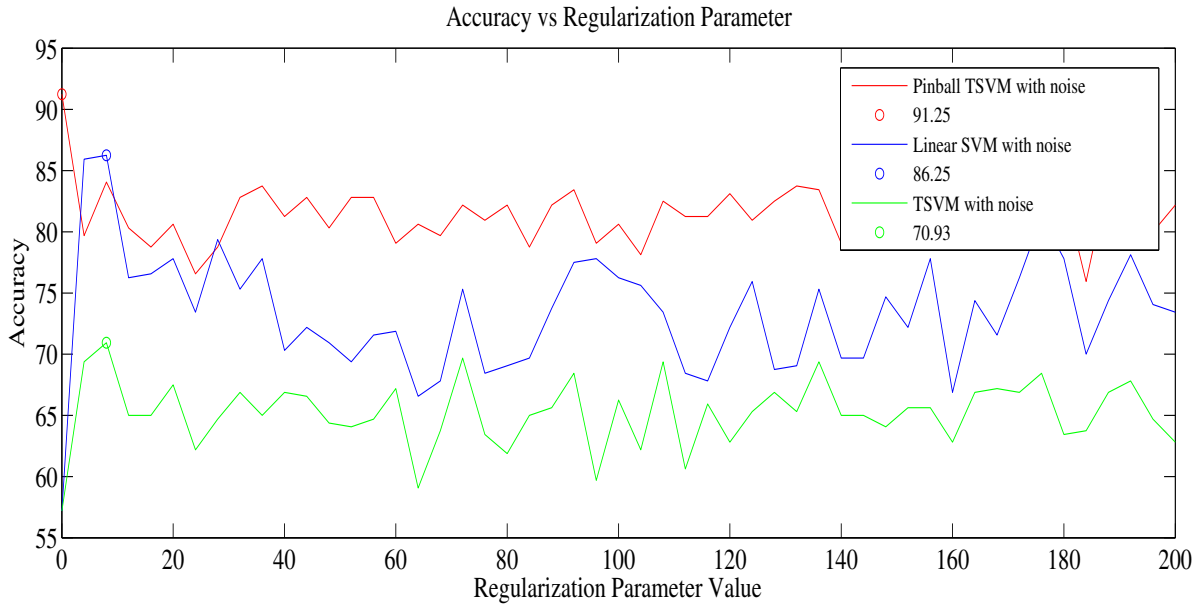

Figure 5.10: Plot of Accuracy versus Regularization Parameter After Adding Noise To The Data Set

when the regularization parameter value is varied. (see Figure 5.10). Therefore, in TWSVM with pinball loss function, strict selection of optimal regularization parameter was not required. For SVM and TWSVM, since the variation in accuracy is more with different regularization parameter values (see Figure 5.10), it is required to select the regularization parameter very carefully.

It should be noted here that all the experiments were performed ten times, corresponding to all three classifiers. To describe the variation in accuracies, box-plots are used. These are shown in Figure 5.11, 5.12 and 5.13. Furthermore, these box-plots also show the variation degradation in accuracies after the addition of Gaussian noise in the feature set.

All the experiments reported above were performed using the linear kernel. The next part is the comparison of all the classifiers for the DR detection problem based on the computation time. The comparison of accuracies of SVM and its variants are shown in the tabular form (see Table 5.1). Comparison are also made based on the CPU

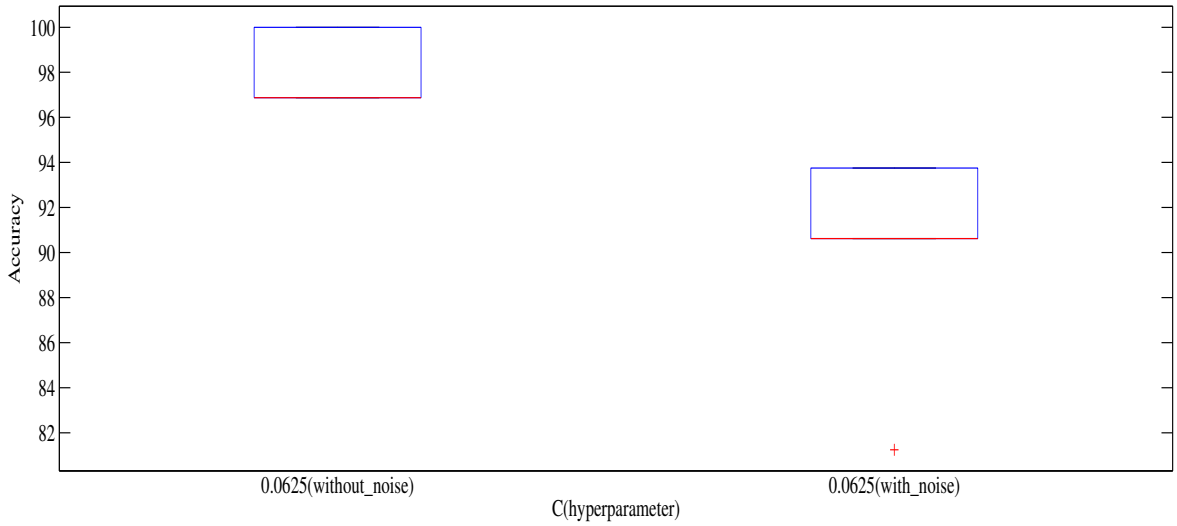

Figure 5.11: Box Plot of Accuracies on Linear SVM

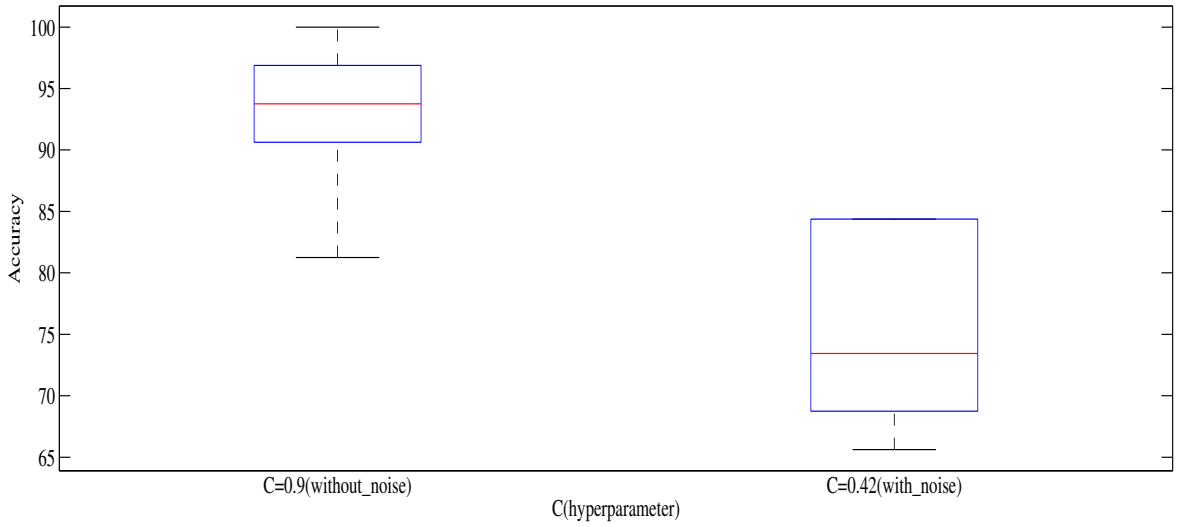

Figure 5.12: Box Plot of Accuracies on TWSVM with Hinge Loss

time consumption. In Table 5.1, the best accuracies and the least time consumptions are shown in bold. Table 5.1 shows that the TWSVM with pinball loss function is an excellent choice for DR detection. It not only classified the images well but also took less computational time to train the model. Another observation is related to

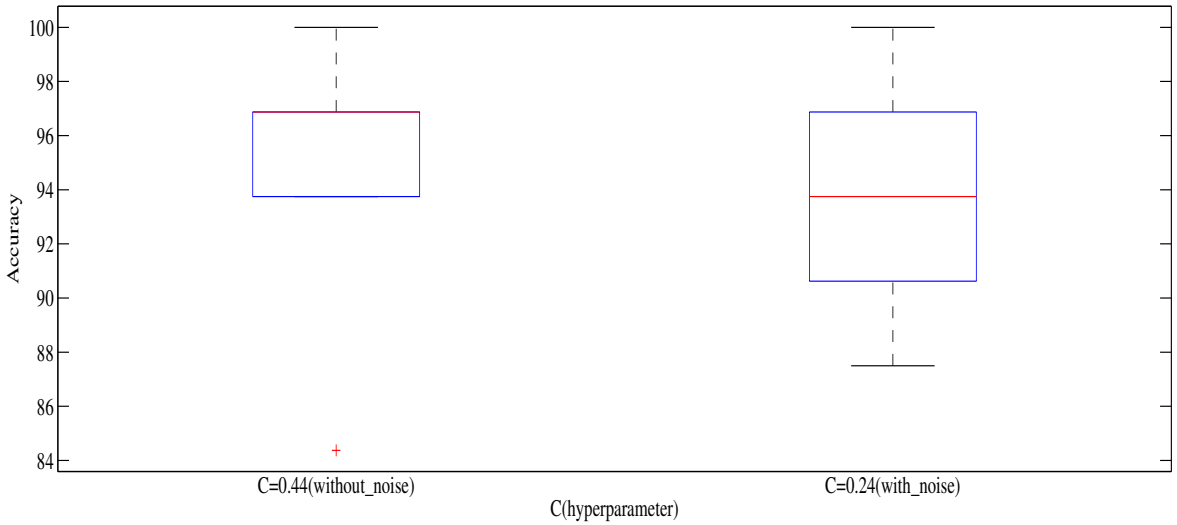

Figure 5.13: Box Plot of Accuracies on TWSVM with Pinball Loss

Table 5.1: Accuracy and Computational Time Of Different SVM Variants On DIARETDB1 Data Set

	Results	Linear SVM	TWSVM with Hinge Loss	TWSVM with Pinball Loss
DIARETDB1 with noise	Accuracy (in %)	93.75	79.06	**94.37**
	Time (in seconds)	6.28	1.76	**0.73**
DIARETDB1 without noise	Accuracy (in %)	97.21	81.56	**98.75**
	Time (in seconds)	4.46	1.73	**1.09**

the robustness of the model. Although the conventional TWSVM got severely affected when the data set was corrupted by Gaussian noise, its robust variant handled the noisy data very well, and the drop in accuracy was less for this model. Sensitivity and specificity are also reported with accuracy on the above-discussed methods in Appendix D (Table 7.2).

In the next section, the work discussed in this chapter is summarized.

5.6 Summary

In this chapter, TWSVM and TWSVM with pinball loss function were used to diagnose diabetic retinopathy detection. To the best of our knowledge, this was the first time that twin SVM was applied to this problem. Also, this work made a comparison with the earlier work of DR detection using SVM. TWSVM with pinball loss function was used for the DR detection problem to make the model robust towards Gaussian noise.

Therefore, the following conclusions can be drawn from this work:

1. TWSVM with pinball loss function for DR detection is the fastest among the above-described classifiers.

2. TWSVM with pinball loss function for DR detection achieves the best accuracy among all the above-described models for noisy data.

3. TWSVM with hinge loss is adversely affected by noise, whereas TWSVM with pinball loss function tolerates the noise very well. This model is also less sensitive to the regularization parameter value choice.

As TWSVM and its variant make the training process computationally fast, this work can be extended to very large datasets as well.

For the DIARETDB1 data set, the pinball loss function with TWSVM performed well in terms of accuracy, but the model loses its sparsity because of the presence of pinball loss function [37]. Therefore, the truncated pinball loss function was proposed [57]. In the next chapter, the truncated pinball loss function is used under a semi-supervised learning framework.